UNMIXING OF MIXTURE PIXEL BASED ON THE CHROMATIC CHARACTERISTICS OF ENDMEMBER SPECTRA

Hui LIN[*], Liangpei ZHANG[**]
[*]The Chinese University of Hong Kong, Shatin, New Territories, Hong Kong
Joint Laboratory for GeoInformation Science
Huilin@cuhk.edu.hk
[**]Wuhan Technical University of Surveying and Mapping,
School of Land Sciences, 430070, P.R.China
Zlp62@public.wh.hb.cn

KEY WORDS: Mixture Pixel, Unmixing, Imaging Spectrometer, Chromatic Characteristics.

ABSTRACT

Unmixing of mixture pixel is a means of determining the relative abundances of materials depicted in hyperspectral imagery based on the materials' spectral characteristics. In linear spectral unmixing theory, the reflectance at each pixel of the image is assumed to be a linear combination of the reflectance of each material (or endmember) present within the pixel. However, in many situations, the endmember spectra are imported from a spectral library or field spectrometer. In order to complete unmixing calculations, these endmember spectra must be pre-processed and convolved to the bandwidths of imaging spectromter in advance. It is very inconvenient and low efficient for the image unmixing calculation. In this paper, authors have developed a new unmixing algorithm based on the linear spectral unmixing theory. The algorithm employs the chromatic characteristics of endmember spectra to unmix the mixture pixels in the hyperspectral remote sensing image. Advantages of the algorithm are the number of required parameters in unmixing calculations is greatly decreased, the speed of unmixing calculation is much faster. The results of unmixing calculation of the algorithm are satisfactory compared with original unmixing method. It is demonstrated the unmixing algorithm developed in this paper can be effectively applied in the classification of imaging spectrometer data.

1 INTRODUCTION

In the processing of remote sensing image classification, mixed pixels are a major source of inconvenience. It is a well known that pixels with more than one land-cover are referred to as mixed pixels while those containing only one type are called pure pixels. Generally, the inconvenience is solved in a way of unmixing pixels to determine the proportions of their component land cover, that is, if each mixed pixel can be decomposed and the proportion of its component cover types (often referred to as "endmembers") determined, the land cover composition of a scene can be estimated through a process known as "unmixing" (Ichoku.C, Karnieli.A, 1996). The usual approach employed to achieve this is through the modeling of spectral mixtures.

The most practicable model of spectral mixtures, now, is a linear mixture model, which is widely used in the classification of imaging spectrometer remote sensing data. In the linear mixture, a pixel contains a number of individual surface components which together contribute to overall pixel level radiance received by a remote detection instrument (Peddle et al., 1999). The spectrum measured by the airborne or satellite sensor can be modeled as a set of endmember spectra, each weighted by the area proportion of material within the sensor IFOV. Thus, the reflectance r_i of a pixel in the ith band is given by

$$r_i = \sum_{j=1}^{n} (r_{ij} x_j) + e_i \qquad (1)$$

with i=1,…,m and j=1,…n where, r_{ij} denotes the reflectance of the jth component of the pixel in the ith spectral band; x_j is the proportion of the jth component in the pixel; e_i is the error term in the ith spectral band. m represents the number of spectral bands while n stands for the number of components in the pixel. Equation (1) can be solved in least

squares technique in order to determine the proportion x_j of the components in individual pixels (Shimabukuro and Smith, 1991).

In order to complete unmixing calculations for equation (1), the endmember spectra are imported from a spectral library, or field spectrometer, or remote sensing image. In calculation, these endmember spectra must be pre-processed and convolved to the bandwidths of imaging spectrometer in advance. It is very inconvenient, low efficient. In addition, calculation process is also time-consumed since there are too many parameters and equations. Therefore, in this paper, our aim is to find out a new fast unmixing algorithm for equation (1).

2 METHOD

It is well known that color is an important parameter in remote sensing applications. It represents a direct and easy accessible information (Mathieu, R., et al, 1998). For this reason, color is often used as basic criteria at different levels in soil classification. However, few papers have reported application of color parameter in classification calculations for imaging spectrometer image data.

According to the CIE 1931 colorimetric system, color of one material is mathematically reproduced with three wavelength-dependent functions: i) the spectral properties of the measured material; ii) the energetic emission of the illumination source under which the material is viewed, and iii) the characteristics of the human eye which acts as a spectral detecting device. For each pixel, which represents one material in a hyperspectral remote sensing image, three stimuli values, X, Y, Z, are first computed with the following CIE equations (Wyszecki and Stiles, 1982):

$$X=\int_{380}^{780} C(\lambda).R(\lambda).\bar{x}(\lambda)\,d\lambda$$

$$Y=\int_{380}^{780} C(\lambda).R(\lambda).\bar{y}(\lambda)\,d\lambda \qquad (2)$$

$$Z=\int_{380}^{780} C(\lambda).R(\lambda).\bar{z}(\lambda)\,d\lambda$$

Where λ is the wavelength, $R(\lambda)$ is the reflectance spectrum of the pixel in the hyperspectral remote sensing image, $C(\lambda)$ is the power density of the lighting source, and $\bar{x}(\lambda)$, $\bar{y}(\lambda)$, $\bar{z}(\lambda)$ are the three modified color matching functions of the CIE 1931 Standard Observer. For a practical calculation of imaging spectrometer data, equation (1) is expressed as

$$X=\sum_{380}^{780} C(\lambda).R(\lambda).\bar{x}(\lambda)\Delta\lambda$$

$$Y=\sum_{380}^{780} C(\lambda).R(\lambda).\bar{y}(\lambda)\Delta\lambda \qquad (3)$$

$$Z=\sum_{380}^{780} C(\lambda).R(\lambda).\bar{z}(\lambda)\Delta\lambda$$

The equation (1) can be rewritten as

$$
\begin{aligned}
r_1 &= r_{11}x_1 + r_{12}x_2 + ...\varepsilon_1 \\
r_2 &= r_{21}x_1 + r_{22}x_2 + ...\varepsilon_2 \\
&..... \\
r_n &= r_{n1}x_1 + r_{n2}x_2 + ...\varepsilon_n
\end{aligned}
\tag{4}
$$

Multiply equation (4) by C(λ), $\bar{x}$ (λ), $\Delta\lambda$

$$
\begin{aligned}
r_1c(\lambda_1)x(\lambda_1)\Delta\lambda &= r_{11}c(\lambda_1)x(\lambda_1)x_1\Delta\lambda + r_{12}c(\lambda_1)x(\lambda_1)x_2\Delta\lambda + ... \\
r_2c(\lambda_2)x(\lambda_2)\Delta\lambda &= r_{21}c(\lambda_2)x(\lambda_2)x_1\Delta\lambda + r_{22}c(\lambda_2)x(\lambda_2)x_2\Delta\lambda + ... \\
&..... \\
r_nc(\lambda_n)x(\lambda_n)\Delta\lambda &= r_{n1}c(\lambda_n)x(\lambda_n)x_1\Delta\lambda + r_{n2}c(\lambda_n)x(\lambda_n)x_2\Delta\lambda + ...
\end{aligned}
\tag{5}
$$

Through equation (5) we can derive

$$
\begin{aligned}
\{r_1c(\lambda_1)x(\lambda_1) + ...r_nc(\lambda_n)x(\lambda_n)\}\Delta\lambda = {} & x_1\{r_{12}c(\lambda_1)x(\lambda_1) + ...r_{1n}c(\lambda_n)x(\lambda_n)\}\Delta\lambda + ... \\
& x_n\{r_{n1}c(\lambda_1)x(\lambda_1) + ...r_{nn}c(\lambda_n)x(\lambda_n)\}\Delta\lambda + \varepsilon_x
\end{aligned}
\tag{6}
$$

$$
\sum_{i=1}^{m} r_ic(\lambda_i)x(\lambda_i)\Delta\lambda = x_1\sum_{i=1}^{m} r_{1i}c(\lambda_i)x(\lambda_i)\Delta\lambda + ...x_n\sum_{i=1}^{m} r_{ni}c(\lambda_{ni})x(\lambda_{ni})\Delta\lambda + \varepsilon_x
\tag{7}
$$

Compare equation (7) with equation (3), then equation (3) can be written as

$$
X = x_1X_1 + x_2X_2 + ... x_nX_n + \varepsilon_x \tag{8}
$$

According to above steps, similarly, we can get

$$
Y = x_1Y_1 + x_2Y_2 + ... x_nY_n + \varepsilon_y \tag{9}
$$

$$
Z = x_1Z_1 + x_2Z_2 + ... x_nZ_n + \varepsilon_z \tag{10}
$$

Compared with equation (4), equation (8), (9), (10) are simpler. But due to limitation of equation number, the number of unknown endmembers in one pixel should be less than or equal to the number of equations for there to be a convenient solution. Since the proportions should sum to unity, the linear constraint, $x_1 + x_2 + ...x_n = 1$ may be included as part of the system of equation, with the proviso that none of the proportions should be negative (i.e. $x_j \geq 0$). This implies that the number of unknown endmembers for equation (8), (9), (10) should be less than or equal to the number of equations, that is, 3 (or 3+1, in the case of inclusion of the sum-to-one linear constraint). Then, x_j 's will be overdetermined in the system of equations, enabling it to be solved by the method of least squares.

Since numbers of endmembers to be solved are restricted to be less than 4 in this new method, if it has wide applications seems questionable. However, researchers have found that over 98 percent of the spectral variation was account for by a linear mixture of three endmembers, green vegetation, shade, and soil. Additional spectral variation appeared as residuals (Gamon, et al, 1993; Vane, et al 1993). Therefore, this unmixing method is reasonable.

3 CALCULATION RESULT

3.1 Data

The airborne imaging spectrometer data used in this case study were acquired in spring 1998 from ShaHe area, in China, by equipment PHI made in China. Some major parameters for PHI are: spectral resolution, 15nm; spatial resolution, 10m. In its flight, total 13 wavebands were selected, which covered from 400nm to 750nm. Before calculation, the internal average relative reflectance calibration (Kruse, F. A. et al, 1988) technique was used to retrieve image spectral reflectance from the raw imaging spectrometer image data.

3.2 Results

According to the algorithm described in previous section, a series of calculations oriented to the imaging spectrometer image data were completed. In calculations, the D65 CIE illuminant (X_n=94.81, Y_n=100.0, Z_n=107.33) standard was used as reference illuminant (Hunt, R, W, G., 1987). This signifies that each material color was calculated as if the material was viewed under average day light. Since no field spectra were collected from the study area during the flight, we selected three endmember spectra directly from the imaging spectrometer image data as reference spectra. They respectively represented spectra of soil, road, building, shown in Fig.1. Their three stimuli values, X, Y, Z, are shown in table 1.

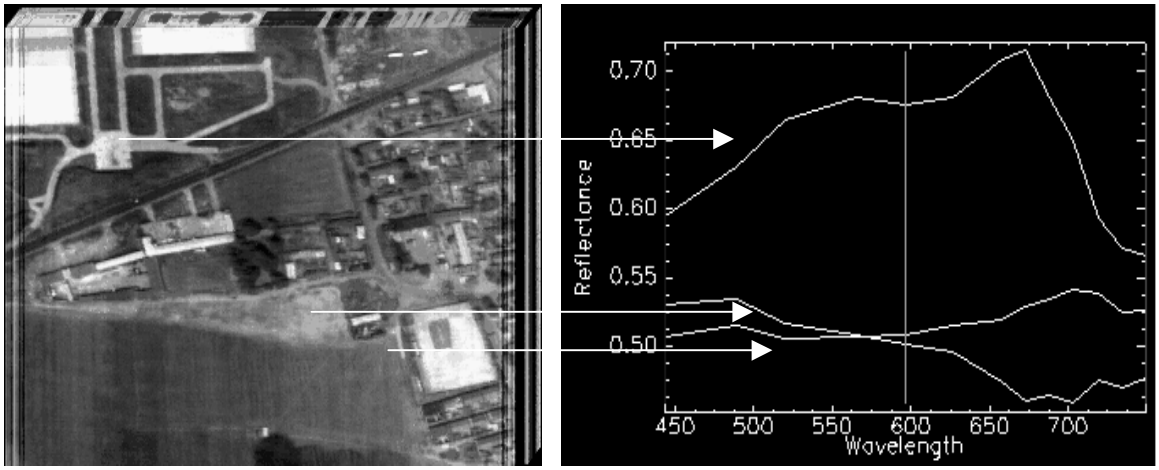

Figure 1, Image cube and endmember spectra

	X	Y	Z
soil	153.998	155.507	07.184
road	145.423	150.288	107.228
building	200.341	202.762	124.357

Table 1, Three stimuli of soil, building, road

Three stimuli value distribution images are also calculated out from imaging spectrometer data. Thus, ummixing results of three endmembers are calculated by the equation (8), (9), (10) with the data from table 1 and the three stimuli distribution images, their results are shown figure 2.

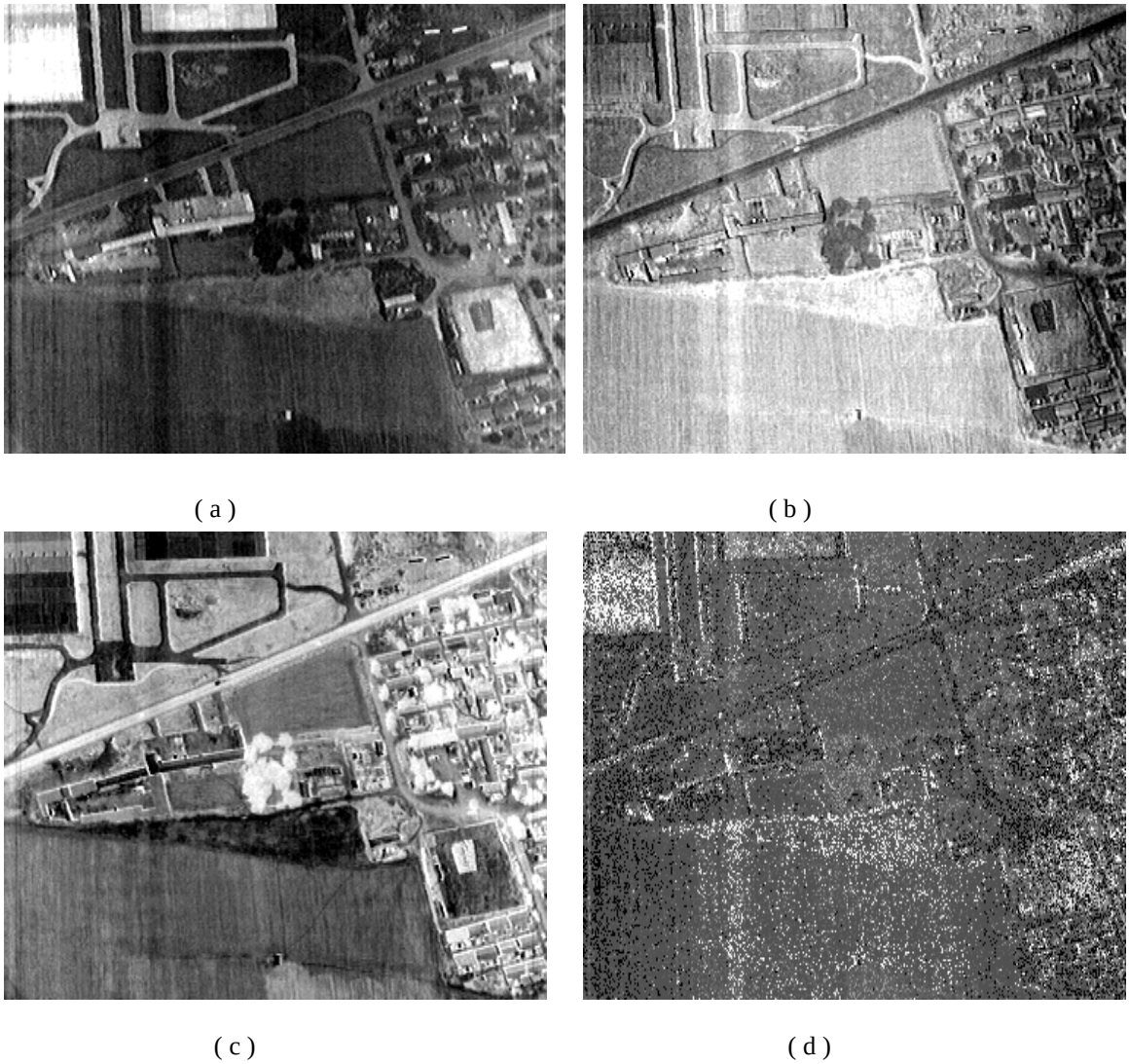

(a) (b)

(c) (d)

Figure 2, Unmixing results for: (a) building; (b) soil; (c) road, and (d) error.

The unmixing results shown in figure 2 have been compared with the results from original linear unmixing method, we find that unmixing results from two different methods are nearly same. But advantages of the algorithm developed in this paper are number of required parameters in unmixing calculations is greatly decreased, speed of unmixing calculation is much faster, residual error is slightly improved better.

4 CONCLUSIONS

In this paper we have developed a new unmixing algorithm based on the chromatic characteristics of endmember spectra. The advantages of this algorithm are number of required parameters in unmixing calculations is greatly decreased, speed of unmixing calculation is much faster, residual error is slightly improved better. But its limits are that only those hyperspectral images from wavelength bands between 380~780nm are applicable in this unmixing processing algorithm, numbers of endmembers in one pixel are not allowed to exceed more than four.

ACKNOWLEDGMENTS

This work was supported by the Nature Science Foundation of China (Grant number: 49701012) and the Surveying and Mapping Foundation of China (Grand number: 98017).

REFERENCES

Gamon, J.A., Field, C.B., Roberts, D.A., Ustin, S.L., and Valentini,R, 1993, Functional patterns in an annual grassland during an AVIRIS overflight, Remote Sens. Environ. 44:239-253

Hunt, R. W. G., (1987), Measuring color. Ellis Horwood Limited, New York, pp186- 192.

Ichoku. C and Karnieli. A, 1996, A review of mixture techniques for sub-pixel land cover estimation, Remote Sensing Reviews, Volume 13, pp.161-186.

Kruse, F. A., Cavin, W. M., (1998), Use of airborne imaging spectrometer data to map minerals associated with hydrothermally altered rocks in the northern Grapevine mountain, Nevada and California, Remote Sens. Environ. 24: 31-51.

Peddle, D.R, Hall, F.G, and Ledrew, E.F, 1999, Spectral mixture analysis and geometric-optical reflectance modeling of boreal forest biophysical structure, Remote Sens.Environ. 67:288-297.

Mathieu, R., Pouget, Pouget, M., Cervelle, B., and Escadafal, R., (1998), Relationships between-based radiometric indices simulated using laboratory reflectance data and typical soil color of an arid environment. Remote Sens. Environ. 66:17-28.

Shimabukuro, Y.E. and Smith, J.A. 1991, The least squares mixing models to generate fraction images derived from remote sensing multispectral data, IEEE Transactions on Geoscience and Remote Sensing 29 (1): 16-20.

Wyszecki,G., and Stiles, W, S., (1982), Color science: concept and methods, quantitative data and formulae. Wiley, New York. 950 pp.

Vane, G., Goetz, A.F.H, 1993, Terrestrial imaging spectrometry: current status, future trends, Remote Sens. Environ. 44:117-126.